Dynamic Characterization of Compliant Materials Using an All-polymeric Split Hopkinson Bar

by O. Sawas, N. S. Brar and R. A. Brockman

ABSTRACT—The split Hopkinson bar is a reliable experimental technique for measuring high strain rate properties of high-strength materials. Attempts to apply the split Hopkinson bar in measurement on more compliant materials, such as plastics, rubbers and foams, suffer from limitations on the maximum achievable strain and from high noise-to-signal ratios. The present work introduces an all-polymeric split Hopkinson bar (APSHB) experiment, which overcomes these limitations. The proposed method uses polymeric pressure bars to achieve a closer impedance match between the pressure bars and the specimen materials, thus providing both a low noise-to-signal ratio data and a longer input pulse for higher maximum strain. The APSHB requires very careful data reduction procedures because of the viscoelastic behavior of the incident and transmitter pressure bars. High-quality stress-strain data for a variety of compliant materials, such as polycarbonate, polyurethane foam and styrofoam, are presented.

Introduction

The conventional split Hopkinson bar (CSHB) is the most widely used method for investigating the dynamic behavior of high-strength materials in the range of strain rate of 100/s to 10,000/s.[1] Much interest has developed recently in providing similar measurements for much more compliant materials such as plastics, rubbers and foams. The mechanical impedance and the wave propagation velocity of CSHB materials (steel, nickel alloy, aluminum alloy, etc.) are extremely large compared to those of most plastics, rubbers and foams. Consequently, serious problems, such as unacceptably high noise-to-signal ratios and short loading time, which limit the maximum achievable strain, arise when CSHB techniques are used to investigate the high strain rate properties of low-density, low-strength materials. This problem is shown in Fig. 1, which presents a typical stress-strain curve at 300/s strain rate for polyurethane foam. Note that the noise-to-signal ratio is high enough to render the stress-strain curve. The CSHB test was discontinued after the specimen was strained to only 8 percent due to limitations on the length of the loading pulse for the CSHB.

In our preliminary studies on high strain rate characterization of compliant materials (polycarbonate and TPOs), it was demonstrated that an all-polymeric split Hopkinson bar (APSHB) can be used to overcome the difficulties associated with the bar-specimen impedance mismatch, as well as short loading pulse duration.[2–4] Polymeric bar materials have better mechanical impedance match than metals with most plastics and foams, and their lower moduli enable them to produce strain gage signals with substantial amplitude that curtails the noise-to-signal ratio problem. In addition, the lower wave propagation velocities in polymeric bars produce longer loading pulse durations that allow sufficient time for specimens to achieve large strain levels. Polymers, however, are viscoelastic in their behavior, which invalidates conventional analyses of CSHB data. Viscoelastic properties of the bar material are needed to properly analyze the experimental strain gage data and relate the data to the specimen stress, strain rate and strain.

Several attempts were made to generalize the split Hopkinson bar technique to use viscoelastic bars. The analysis of the viscoelastic bar data varies in difficulty and complexity depending on the assumptions made. Zhao *et al.*[5–7] proposed a three-dimensional analytical solution of the longitudinal wave propagation in a linear viscoelastic bar. They calculated the forces and the particle velocity at the specimen interface from the measured strain by the Fourier analysis. Their approach required that the complex modulus of the bar material be known, and that all the analyses be done in the frequency domain.

Wang *et al.*[8] used a simple three-element linear viscoelastic model to describe the linear viscoelastic behavior of the pressure bar material. The one-dimensional assumption that they adopted and their simple model allowed them to use the method of characteristics to solve the resulting linear viscoelastic wave propagation equations. Unfortunately, their study does not report stress-strain data for any material usable for evaluating their approach.

Theoretical Analysis

The stress, strain and strain rate of the specimen in a compressive split Hopkinson bar test are determined from the bar stress $\sigma(x, t)$ and the bar particle velocity $v(x, t)$ at the bar-specimen interface as shown in Fig. 2 using the following equations:[9]

$$\sigma_s(t) = \frac{A_b}{A_s}\sigma_t(x_2, t) \tag{1}$$

$$\dot{\varepsilon}_s(t) = \frac{2}{l_s}v_r(x_1, t) \tag{2}$$

$$\varepsilon_s(t) = \frac{2}{l_s}\int_0^t v_r(x_1, t)dt, \tag{3}$$

O. Sawas is Postdoctoral Fellow, N. S. Brar is Research Physicist and R. A. Brockman is Professor and Senior Researcher, University of Dayton Research Institute, Dayton, OH 45469-0182.

Original manuscript submitted: November 11, 1997.

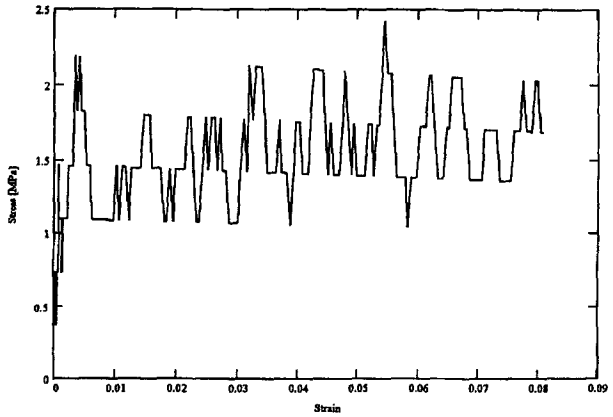

Fig. 1—Typical stress-strain curve for polyurethane foam obtained using the CSHB

where A_b, A_s are the bar and specimen cross-sectional area and l_s is the specimen gage length.

To relate the stresses, strains and particle velocities at the specimen-bar interface of the bar to those at the strain gage location, the stress-strain relationship, strain-particle velocity relationship and solution of the one-dimensional wave propagation equation for a thin, semi-infinite circular rod are needed.

CSHB

In this case, the pressure bars are made from elastic material (steel, aluminum alloy, etc.). The solution of the one-dimensional elastic wave propagation problem for a thin, semi-infinite circular rod indicates that a strain, stress or displacement pulse propagates along a thin, semi-infinite bar without dispersion or attenuation.[10–12] The absence of attenuation in the propagated wave implies that the values of stresses, strains and particle velocities at the specimen-bar interface can be replaced by those measured at the strain gage locations. Using the elastic stress-strain and strain particle velocity relationships together with the information from the solution of the elastic wave propagation in a thin bar, eqs (1) through (3) reduce to

$$\sigma_s(t) = E\frac{A_b}{A_s}[\varepsilon_t(x_{g2}, t)] \tag{4}$$

$$\dot{\varepsilon}_s(t) = \frac{-2C}{l_s}[\varepsilon_r(x_{g1}, t)] \tag{5}$$

$$\varepsilon_s(t) = \frac{-2C}{l_s}\int_0^t [\varepsilon_r(x_{g1}, t)]dt, \tag{6}$$

where E is the elastic modulus and C is the elastic wave propagation velocity in the bar material.

APSHB

In the case where the pressure bars are made from viscoelastic material, the following steps must be taken to determine the specimen stress, strain rate and strain from the strain measured at the strain gage location on the pressure bars:

1. Determine the viscoelastic properties of the polymeric pressure bar material employed in the APSHB.

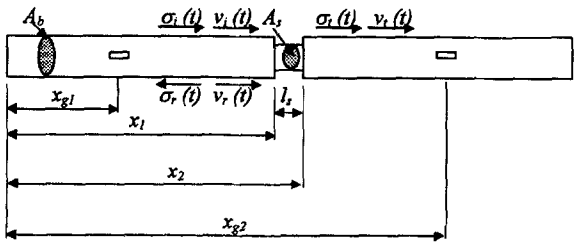

Fig. 2—Split Hopkinson bar configuration showing incident, transmitted and reflected pulses

2. Using the predetermined material properties, solve the resulting linear viscoelastic wave propagation equations in terms of strain.
3. Using the solution of the linear viscoelastic wave propagation in terms of strain, determine the strain $\varepsilon(x_{1,2,},t)$ at the bar-specimen interface from the strain $\varepsilon(x_{g1,g2,},t)$ measured at the strain gage locations.
4. Based on material properties of the pressure bars, establish relationships between strain, stress and particle velocity in the viscoelastic pressure bar.
5. Using the stress-strain relationship, determine the stress $\sigma(x_{1,2,},t)$ at the bar-specimen interface from the predetermined strain $\varepsilon(x_{1,2,},t)$.
6. Using the strain-particle velocity relationship, determine the particle velocity $v(x_1,t)$ at the bar-specimen interface from the predetermined strain $\varepsilon(x_{1,},t)$.
7. Substitute the values of the predetermined stress and particle velocity at the bar-specimen interface into eqs (1) through (3) to obtain the specimen stress, strain rate and strain.

Viscoelastic Properties of the Polymeric Pressure Bars

It is important to determine very accurately the viscoelastic properties of the pressure bar material used in the APSHB apparatus. Since the Hopkinson bar experiment is dominated by the wave propagation phenomena, a wave propagation method was adapted to determine the linear viscoelastic properties of the polymeric bar materials. The wave propagation method used for this study is based on the work of Kaya.[13] This method can be used to either determine the material linear viscoelastic properties (identification problem) or solve linear viscoelastic wave propagation in material with known linear viscoelastic properties (prediction problem). For the identification problem, the method requires measurements of a single quantity such as strain or particle velocity at two different locations along a bar that is overrun at different times by the propagating wave. These measurements can then be related analytically to the viscoelastic material properties. The development of the procedure requires the mathematical formulation of the linear viscoelastic wave propagation in semi-infinite circular rods. This formulation and a detailed derivation of the procedures are presented in Refs. 13-15. The following are the major steps of this method as applied to the identification problem:

1. Use the solution of the linear viscoelastic wave propagation equation to establish a relationship between two

strain pulses measured at two locations along a linear viscoelastic bar. The two signals must be time shifted first so that both originate at their local time origins (i.e., the times when the wave fronts each reach the strain gage location). The resulting relationship then can be solved for the auxiliary function $S_R(t)$ that relates the two strain pulses. This function will be used to reconstruct the strain pulse at the bar-specimen interface from the measured pulses at the strain gage locations.

2. Establish a relationship between the auxiliary function $S_R(t)$ and the time derivative of the function $m(t)$ that relates strain to particle velocity. The resulting equation is then solved for the function $\dot{m}(t)$.
3. Integrate the function $\dot{m}(t)$ to obtain $m(t)$. This function will be used later to determine the particle velocity from the measured strain.
4. Establish an analytical relationship between $m(t)$ and the relaxation function $J(t)$, and solve the resulting equation to determine the function $J(t)$.
5. Solve for the creep function $G(t)$. This function will be used to determine stresses from the measured strain.

The major steps of this method as applied to the property identification problem are shown in the chart given in Fig. 3.

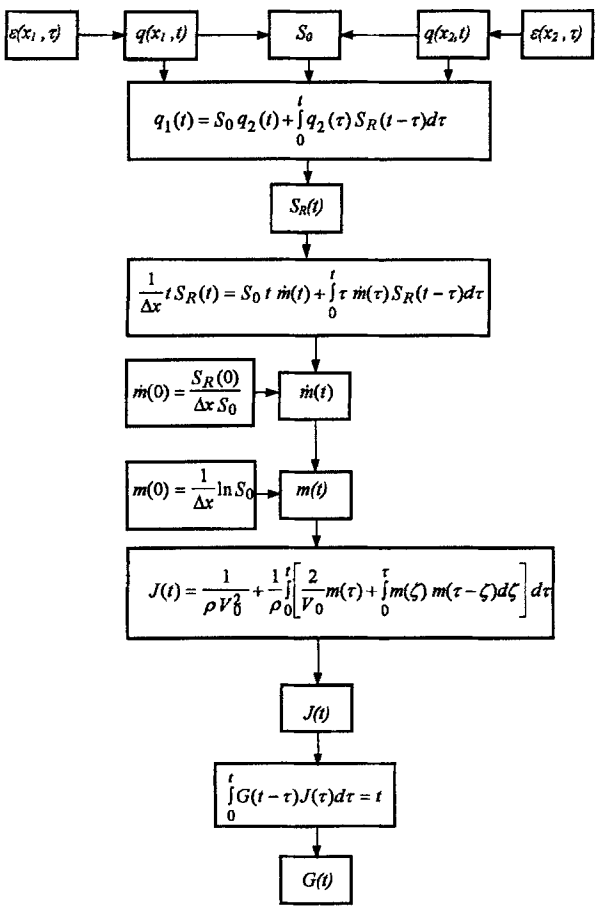

Fig. 3—Flowchart showing the major steps in the identification problem

Experimental Configuration to Identify Viscoelastic Properties

The experimental configuration used to determine the viscoelastic properties of the polymeric bars is shown in Fig. 4. The 25.4-mm diameter bars were instrumented with strain gages at four locations. At each location, two gages were oriented axially and were bonded to opposite sides of the bar. Each pair was connected to opposite legs of a sensing bridge circuit to cancel any bending disturbance. Data were collected digitally at 1-μs intervals using a digital oscilloscope. Each bar was calibrated individually for its viscoelastic properties. Typical strain gage profiles from gages 1 and 2 are shown in Fig. 5. It is clear that the shape and magnitude of the pulses change as the pulses propagate along the bars.

Wave propagation tests were performed on each cast acrylic bar considered a candidate for APSHB to determine its very early time viscoelastic properties. Data collected from these tests were used to determine the viscoelastic properties of the pressure bars and to validate the viscoelastic linearity approximation over the operational ranges of stress and strain levels, as well as to compare the properties of the incident and the transmitter bar materials. The accuracy of the viscoelastic model obtained from these tests is evaluated by reconstructing the first strain gage profile from the profile of the second strain gage positioned 1.12 m away and the material properties determined earlier. Comparison of the computed and observed versions of the first strain gage pulse shown in Fig. 6 reveals the accuracy of the analysis.

To determine whether the viscoelastic material behaves linearly (i.e., the material properties are not functions of strain level), 21 tests were performed on the transmitter bar at nine strain levels between 3×10^{-4} and 3×10^{-3} with two replications at each strain level. These different strain levels span the range likely to be encountered during APSHB use. The creep and relaxation functions $J(t)$ and $G(t)$ were determined for

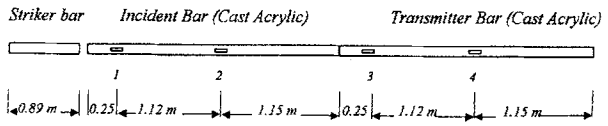

Fig. 4—Schematic sketch of the material identification test configuration

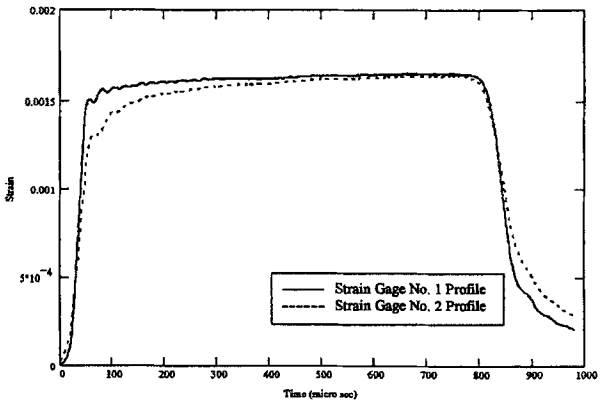

Fig. 5—Observed profiles from strain gages 1 and 2 on the cast acrylic incident bar

each strain level. Figure 7 shows a comparison of the relaxation functions $G(t)$ obtained at different strain levels.

Starting time of each of the two strain signals used to determine the material properties is very critical. Any relative shift between the two signals could induce a large error in the result. The risk of such shift can be significantly reduced if the time difference between the two gage records is determined from gage separation and the viscoelastic wave propagation velocity.

Data obtained from tests for strain levels between 3×10^{-4} and 3×10^{-3} (approximately between 1.0 and 10 MPa) strongly suggest that the materials behave in a linear viscoelastic manner over the strain range investigated.

APSHB Experimental Configuration and Test Procedures

The APSHB shown in Fig. 8 was constructed from cast acrylic bars 25.4 mm in diameter. Incident and transmitter bars were nearly 2.5 m long, with strain gage pairs mounted near the center of each bar. The two pressure bars were mounted and aligned longitudinally in Teflon bushings that supported them rigidly along a single horizontal axis while permitting free axial movement. Test specimens were placed between the two bars. High-strength titanium alloy anvils (0.6 mm thick) were placed between the specimen and the two bars (as shown in Fig. 8) to prevent damage to the bars during

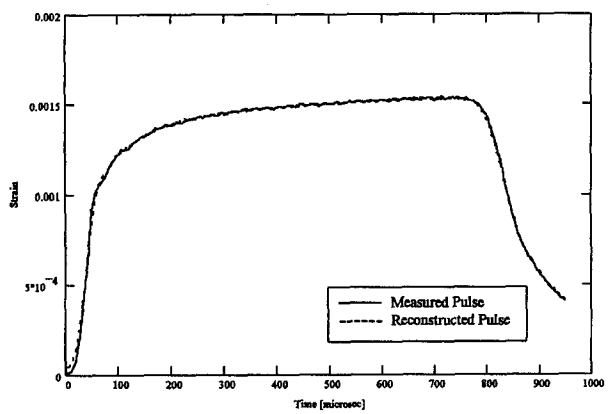

Fig. 6—The reconstructed pulse as predicted from the second pulse and $S_R(t)$

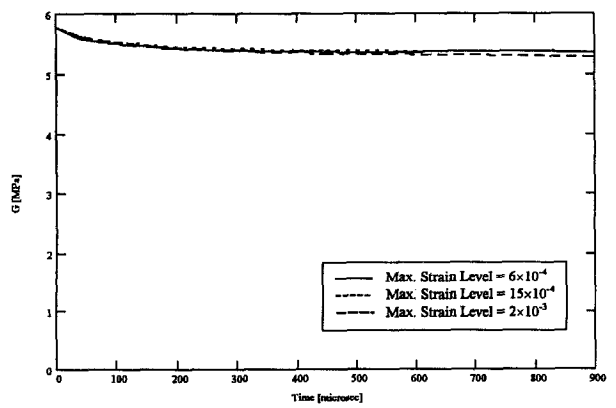

Fig. 7—Result for the relaxation function $G(t)$ obtained at different strain levels

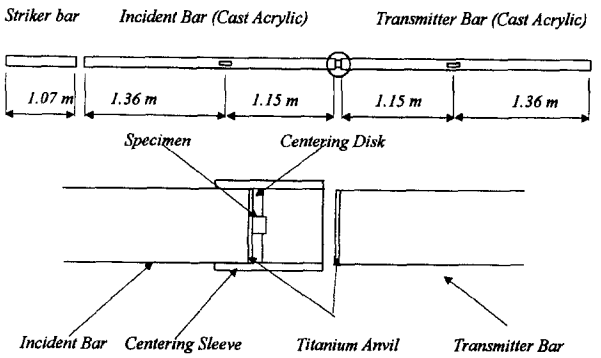

Fig. 8—Schematic of the all-polymeric split Hopkinson bar configuration

specimen compression and to minimize localized elastic deformation at the specimen-bar interface. The specimen-anvil interface is lubricated before each test with petroleum jelly to reduce friction and allow radial expansion of the specimen. To minimize bending in the transmitter bar caused by misalignment between the specimen and the bar axes, all test specimens were aligned with the centers of the bars using a centering disk arrangement shown in Fig. 8. The centering disk was removed prior to testing; petroleum jelly was used to hold the specimens in the proper position. The 1.07-m long striker bar was accelerated to the desired impact velocity by a slingshot mechanism in which the driving force was supplied by a torsion bar spring. This spring-loaded mechanism was cocked using a hydraulic piston and released by controlled failure of a shear pin. Adjusting the drawback of a launch plate connected to the torsion bar controlled the velocity of the striker bar. The amplitude of the compressive pulse produced by the striker bar impact was directly proportional to the striker bar velocity V_s. Tests were performed in a temperature- and humidity-controlled environment. The test conditions were similar to those used to determine the viscoelastic properties of the polymeric bars.

APSHB Data Reduction

Strain gage data obtained from the APSHB tests described in the previous section were analyzed using the following procedures. In the configuration shown in Fig. 8, only the incident and the transmitted pulses are used. The transmitted stress $\sigma_t(x_2, t)$ and the reflected particle velocity $v_r(x_1, t)$ at the specimen-bar interface can be determined from the strain data $\varepsilon_i(x_{g1}, t)$, $\varepsilon_t(x_{g2}, t)$ collected at the gage locations following these steps:

1. The strains $\varepsilon_t(x_2, t)$ and $\varepsilon_i(x_1, t)$ at the specimen-bar interface were determined from those at the strain gage location $\varepsilon_t(x_{g2}, t)$ and $\varepsilon_i(x_{g1}, t)$ using (see Fig. 3)

$$\varepsilon(x_1, t) = S_0\varepsilon(x_{g1}, t) + \int_0^t \varepsilon(x_{g1}, t)S_R(t-\tau)d\tau \tag{7}$$

$$\varepsilon(x_2, t) = S1_0\varepsilon(x_{g2}, t) + \int_0^t \varepsilon(x_{g2}, t)S1_R(t-\tau)d\tau. \tag{8}$$

2. The two functions $S_R(t)$ and $S1_R(t)$ may be determined either directly from wave propagation tests or indirectly from the solution of a prediction problem starting from the material property $G(t)$ or $J(t)$ and the distance between the specimen-bar interface and the strain gage location (Δx). To minimize the error due to numerical approximation in the indirect approach, both $S_R(t)$ and $S1_R(t)$ are determined directly from the wave propagation experiments described in the previous section.
3. The stresses at the specimen-bar interface $\sigma_t(x_2, t)$ are determined from the strain $\varepsilon_t(x_2, t)$ at strain gage locations using

$$\sigma(x_2, t) = \varepsilon(x_2, 0)G(t) + \int_0^t G(t-\tau)\frac{\partial \varepsilon(x_2, \tau)}{\partial \tau} d\tau. \tag{9}$$

4. The reflected strain $\varepsilon_r(x_1, t)$ is determined from

$$\varepsilon_i(x_2, t) + \varepsilon_r(x_1, t) = \varepsilon_t(x_1, t). \tag{10}$$

5. The reflected particle velocity $v_r(x_1, t)$ is determined by solving the integral equation

$$-\varepsilon_r(x_1, t) = \frac{v(x_1, t)}{V_0} + \int_0^t v_r(x_1, \tau)m(t-\tau)d\tau. \tag{11}$$

The results from eqs (9) and (11) are substituted into eqs (1) through (3) to obtain the specimen stress, strain rate and strain. Since the method of determining the reflected pulse used to calculate the specimen strain rate and strain involves subtraction of one measured signal from another, any relative time shift between the two signals introduces error into the specimen strain rate and strain determinations. Such time shifts are very hard to avoid because it is difficult to determine precisely the starting time of each pulse from the noisy background. To reduce the possibility of such a shift occurring, very precise values of the wave propagation velocity in the bar, the distance between the incident and transmitter strain gages and the wave propagation velocity in the specimen material are required. When these values are obtained, the beginning of the transmitted pulse can then be determined from the beginning of the incident pulse by adding to it the predetermined time required for the pulse to propagate between the two gages and through the specimen. This time shift value is used regardless of the actual value of the transmitted signal, which can be affected by the scope presetting and strain gage noise.

Validation of the APSHB Data Reduction Procedures

Sixteen tests were performed on aluminum 1100 (Al 1100) to validate the APSHB viscoelastic data analysis. The first eight tests were conducted with the CSHB at strain rates of 400/s, 1000/s and 4000/s. The results show conclusively that this material is strain rate insensitive over the range investigated. Identical specimens were then tested with the APSHB at nominal strain rates of 500/s, 1000/s and 1500/s. Stress-strain results for one typical test at a strain rate of 1000/s are presented in Fig. 9. The solid curve represents our best estimate of Al 1100 stress-strain from the CSHB. The lowest curve represents the raw strain gage data obtained from the APSHB analyzed assuming that the polymeric bar behaves elastically. Note that this curve underpredicts the stress by about 15 percent and overpredicts the strain by more than 26 percent. The third curve represents the APSHB results that were analyzed by the viscoelastic analysis described earlier. This comparison confirms that the APSHB data and the viscoelastic data reduction model are very accurate.

The close similarities of the CSHB and APSHB results are very important. The similarities demonstrate sufficiently the effectiveness of APSHB configuration with regard to accuracy and reliability.

Results

Three materials with notably high compliance were tested using the APSHB technique. The tested materials are important for many engineering applications and were chosen to cover wide ranges of densities (50-1200 kg/m^3) and strengths (1-300 MPa). Some materials, like polycarbonate, can be characterized to some extent using both the CSHB and the new APSHB, yet the data quality and maximum strain levels achievable with the APSHB far exceed the capabilities of any CSHB yet constructed. High strain rate data on materials such as styrofoam, on the other hand, can only be obtained using the APSHB technique.

Polycarbonate

Nine room temperature dynamic compression tests were performed on generic polycarbonate specimens using the APSHB. Three different strain rates were investigated, with three replications at each test condition. Test specimens were 3.2 mm in diameter and 3.2 mm long. The quality of the data in terms of signal-to-noise ratio is dramatically improved compared to that obtained from the CSHB. Additionally, the maximum achievable strain is increased by a factor of three, mainly due to the longer pulse duration that can be generated and accommodated in the cast acrylic bars.

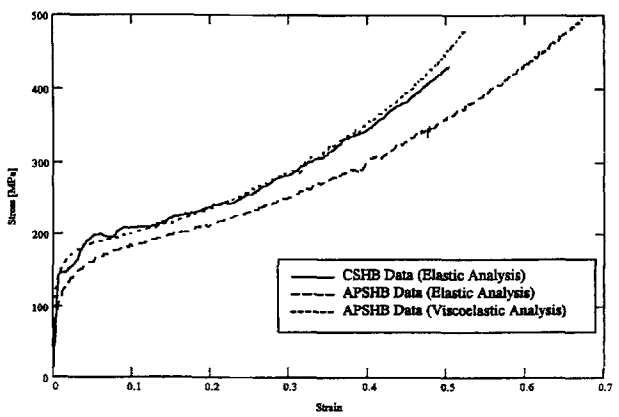

Fig. 9—Comparison of the data on Al 1100 specimen obtained using conventional split Hopkinson bar and all-polymeric split Hopkinson bar following elastic and viscoelastic analyses

Strain rate effects on the mechanical stress-strain behavior of polycarbonate can be determined by comparing the stress-strain curves produced at several strain rates. Figure 10 shows engineering stress-strain curves for polycarbonate at three strain rates: 500/s, 1200/s and 1700/s. The stress at 0.1 engineering strain increases from 115 MPa at 500/s strain rate to 120 MPa at 1200/s and 128 MPa at 1700/s. This consistent behavior suggests that polycarbonate is sensitive to strain rate to a significant degree. The present data for polycarbonate at a strain rate of 1700/s were compared to the data reported by Walley and Field[16] at a strain rate of 1980/s obtained using the drop weight testing technique with high-speed photography.

Polyurethane Foam

The low-density, low thermal conductivity and high-energy absorption capabilities of most foams make them first choices for many engineering applications. The interior padding and trim of both civilian and military vehicles are examples of their modern use. High strain rate data for these materials are needed to numerically simulate various types of high strain rate phenomena such as transportation vehicle crashes, occupant head and knee impact on the vehicle interior and so on. These data are impossible to obtain from the CSHB because of the large impedance mismatch between the polyurethane foam and the bar material. Specimens of 12.7 mm in diameter and 12.7 mm long were machined from 25.0-mm thick plates. Four tests were performed on these specimens using the APSHB at strain rates of 450/s, 800/s, 1050/s and 1350/s with one test at each strain rate. Two more tests were performed at quasi-static strain rates of 0.001/s and 0.2/s using a conventional Universal test machine, and the data are compared in Fig. 11. The extensometer range limited maximum strain of 0.26 achieved in the quasi-static test. The consistent increase in the stress levels as the strain rate increased from 0.2/s to 1350/s is a strong indication of the strain rate sensitivity of polyurethane dynamic behavior.

Styrofoam

To further demonstrate the capabilities of the APSHB, styrofoam, an extremely low-density, low-strength material, was characterized using the APSHB. This material is widely used in product packaging and protective helmets. Specimens 12.7 mm in diameter and about 2 mm thick were punched from the bottom of styrofoam coffee cups. Eight tests were performed at four strain rates of 600/s, 1150/s, 1750/s and 2300/s, with two replications at each strain rate. Stress-strain curves obtained from the tests are compared in Fig. 12. The data again suggest that styrofoam has mechanical properties that are strain rate dependent, especially at high strain rates. No known method other than the APSHB is capable of measuring such compliant material at strains and strain rates in the range appearing in Fig. 12.

Conclusions

The present work demonstrates that split Hopkinson bar technology can be extended by using an APSHB to measure high strain rate characteristics of low-density, low-strength materials such as plastics, rubbers and foams. A novel experimental technique and associated data reduction procedures have been developed which provide accurate stress-strain data for such materials and eliminate the many problems associated with conventional split Hopkinson bar technology. The validity of the test method and the viscoelastic data reduction procedures have been demonstrated for materials which are both strain rate sensitive and strain rate insensitive. They also have been shown to produce very accurate data which contain minimum noise and artificial oscillations.

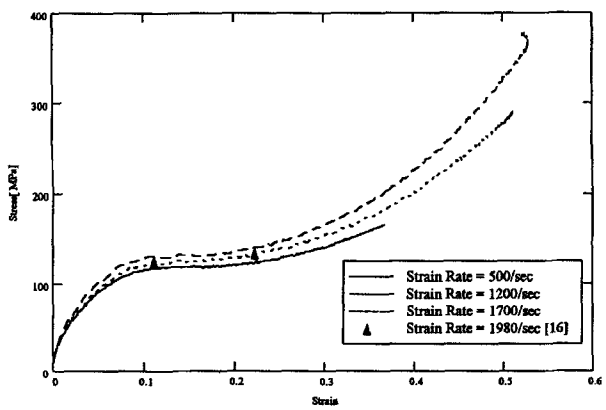

Fig. 10—Stress-strain curves for polycarbonate at three different strain rates

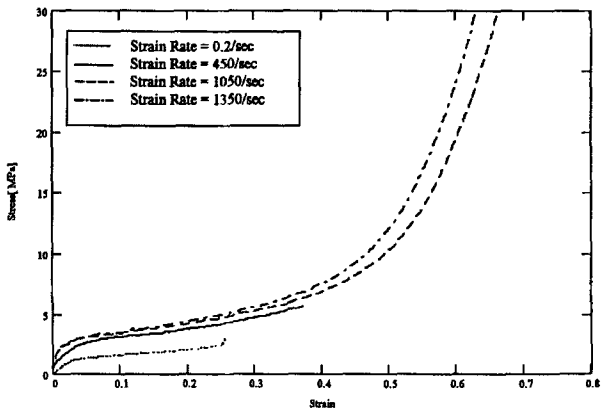

Fig. 11—Stress-stain data for polyurethane foam obtained at four strain rates

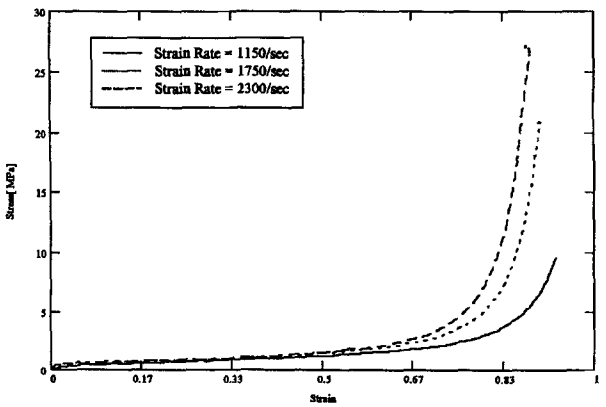

Fig. 12—Stress-stain data for styrofoam obtained at three strain rates

References

1. Nicholas, T., Impact Dynamics, ed. J.A. Zukas, T. Nicholas, H.L. Swift, L.B. Greszczuk, and D.R. Curran, Krieger, Malabar, FL (1992).

2. Ramamurthy, A.C., Brar, N.S., and Sawas, O., "Deformation and Fracture of Thermopolyolefins (TPO) Plastics at High Strain Rates, Split Hopkinson Bar Experiments, a Preliminary Study," Ford Motor Company, Detroit, MI (June 1994).

3. Ramamurthy, A.C., Sawas, O., and Brar, N.S., "Deformation and Fracture of Thermopolyolefin (TPO) Plastics at High Strain Rates," Advanced Coatings Technology Conference, Detroit, MI (November 1994).

4. Sawas, O., Brar, N.S., and Ramamurthy, A.C., "High Strain Rate High/Low Temperature Response of Plastics," Shock Compression of Condensed Matter-1995, ed. S.C. Schmidt and W.C. Tao, American Institute of Physics, New York (1994).

5. Zhao, Z. and Gary, G., "A Three Dimensional Analytical Solution of the Longitudinal Wave Propagation in a Finite Linear Viscoelastic Cylindrical Bar. Application to Experimental Technique," J. Mech. Phys. Solids, **43** (8), 1335 (1995).

6. Zhao, Z., Gerard, G., and Klepaczko, J.R., "On the Use of Viscoelastic Split Hopkinson Pressure Bar," Int. J. Impact Eng., **16** (1), 1 (1996).

7. Zhao, Z. and Gerard, G., "On the Use of SHPB to Determine the Dynamic Behavior of Materials in the Range of Small Strain," Int. J. Solids Struct., **33** (23), 3363 (1996).

8. Wang, L., Labibes, K., Azari, Z., and Pluvinage, G., "Generalization of Split Hopkinson Bar Technique to Use Viscoelastic Bars," Int. J. Impact Eng., **15**, 669 (1994).

9. Kolsky, H., "An Investigation of the Mechanical Properties of Materials at Very High Strain Rates of Loading," Proc. Roy. Soc. B, **62**, 676 (1949).

10. Follansbee, P.S., "The Hopkinson Bar in Material Testing," Metals Handbook 8, ASM, Metal Park, OH, 9th ed., 198 (1985).

11. Meyers, M.A., Dynamic Behavior of Materials, John Wiley & Sons, New York (1994).

12. Graff, K.F., Wave Motion in Elastic Solids, Dover (1975).

13. Kaya, I., "Very Early Time Characterization of Linear Viscoelastic Material," Ph.D. thesis, University of California, Berkeley (1968).

14. Sawas, O., "High Strain Rate Characterization of Low-density Low-strength Materials," Ph.D. thesis, University of Dayton (1997).

15. Sawas, O., Brar, N.S., and Brockman, R.A., "High Strain Rate Characterization of Plastics and Foams Using Polymeric Spit Hopkinson Bar," APS 1997 Topical Conference on Shock Compression of Condensed Matter, Amherst, MA (July 27-August 1 1997).

16. Walley, S.M. and Field, J.E., "Strain Rate Sensitivity of Polymers in Compression from Low to High Rates," DYMAT J., **1**, 211 (1994).